Energy Proceedings
Vol 27, 2022
ISSN 2004-2965

Technology for efficiently converting energy stored in low-pressure compressed air to ensure security of electricity supply

Jacek Leszczyski[1], Dominik Gryboś[2*], Jan Markowski[1]

1 AGH University of Science and Technology, Faculty of Energy and Fuels, Department of Thermal and Fluid Flow Machines, Cracow, Poland

2 AGH University of Science and Technology, Faculty of Energy and Fuels, Department of Thermal and Fluid Flow Machines Cracow, Poland (Corresponding Author)

ABSTRACT

The growing interest in ecological energy sources is driving the dynamic development of energy storage. Increasing the efficiency of compressed air energy storage is associated with the efficiency of energy utilisation. This paper shows the possibilities of developing an energy utilisation component such as the compressed air engine. The authors present simulation results that show better engine performance when using a three-cylinder solution.

Keywords: compressed air energy storage, wastes of energy, hybrid storage, energy recovery, compressed air energy system, low-pressure air engine

NOMENCLATURE

Abbreviations	
CAES	Compressed Air Energy Storage
CAE	Compressed Air Engine
CA	Compressed Air
i-CAES	Isothermal Compressed Air Energy Storage
PMSG	Permanent Magnets Synchronous Generator
Symbols	
A_1	piston surface, m2
A_2	piston rod surface, m2
F	force, N
F_T	Coulomb-Viscous friction force, N
I	current, A
J	moment of inertia
Lg	load resistance, Ω
M	rotary torque, Nm
M_F	fraction torque, Nm
M_{Ind}	braking torque of the bearing - load-independent, Nm
M_{dep}	braking torque of the bearing - load-dependent, Nm
M_G	generator torque, Nm
N	piston contact force, N
N_{pb}	poles number, -
P	power, W
P_{eq}	equivalent load, Nm
R	stator winding resistance of PMSG, Ω
R_g	stator winding inductance of PMSG, H
P_{gen}	electric power, W
P	power of the engine
P_{air}	power of compressed air, W
$\dot{V}$	volumetric expenditure, $\frac{m^3}{s}$
d_m	bearing pitch diameter, m
f_0	factor depending on the type and size of the bearing and the type of lubrication,
f_1	the factor depending on the type and size of the bearing and the acceptable static load factor,
l	connecting rod length, m
p_A	supply pressure, bar
p_0	absolute pressure, bar
p_1	supply pressure in the first chamber of the cylinder, bar
p_2	supply pressure in the second chamber of the cylinder, bar
r	crank length, m
u	piston velocity, m/s
α	

β	alpha, rad
η	betta, rad
ω	efficiency, [%]
μ_1	omega, RPM
μ_2	static friction coefficient,
μ_3, μ_4	dynamic friction coefficient,
Ψ	vicious friction coefficients,
v	magnetic flux, Wb
t	kinematic viscosity of the oil
	time, s

1. INTRODUCTION

Nowadays, due to the intermittent supply of energy by wind or solar farms, energy storage systems have gained popularity [3].

Depending the moment, due to energy storage, we can generate potential energy in a very advantageous and economical way or use it upon demand [5].

We can distinguish the following types of energy storage systems: electrochemical (converts chemical energy into electrical energy) [20], chemical (energy released based on a chemical reaction) [21], electricity (capacitor, supercapacitor, and magnetic energy storage) [22], thermal (stores heat or cold in a storage medium at a temperature for further use) [22] and mechanical (converts mechanical work into electricity) [1]. One mechanical storage system is Compressed Air Energy Storage (CAES). CAES can play a huge role in maintaining the continuity of energy supply in the energy system [11]. As an energy storage system, CAES can help reduce fluctuations in the energy market [27].

CAES consists of the following elements: a compressor, a storage tank, and a utilisation component. The storage is charged by compressors converting electricity into potential energy of compressed air. Electricity is generated by expanding the air through the utilisation component [3].

In this paper [27], a high-pressure compressor for CAES systems was analysed. The selection of the optimal inlet pressure and proper control of the piston movement can lead to the highest energy efficiency of the device [27].

Storage tanks can be isobaric or isochoric. Isobaric storage tank systems are known to gain efficiency and energy density [18]. Using an isobaric tank provides constant supply pressure and can develop the whole functioning of the system. In paper [12], the authors show an innovative solution of constant pressure tanks used for carbon dioxide storage in this case. By using two tanks (low and high pressure), they manage to sustain constant pressure, so there is no need to use throttling valves to control pressure value. By avoiding throttling valves in the expansion system, efficiency values increase due to not generating local losses.

In work [13], the compressed air tank at constant pressure is based on a variable storage volume. There was an increase in the efficiency of the system obtained from 45.8% to 52.9% after replacing the isochoric tank with an isobaric one. The losses of both tanks do not affect the overall efficiency. Still, the isobaric tank works better with other system components. The authors emphasise that pressure regeneration behind the actuator is necessary to obtain even higher system efficiency.

The nature of compressed air storage also allows us to locate the tank in any location. Compressed gas can be stored in above-ground, underground or underwater tanks [6],[14], [15].

The use of isochoric systems requires the application of throttling valves. In order to limit losses, we should use a reducer with the lowest loss coefficient. Research has shown that energy losses within the throttle valve can be as high as 5,14%, depending on the temperature and system operating parameters [17].

CAES has many advantages such as viability and ease of use of the storage system, high capacity, low cost per kWh, and minor needs for power electronic converters. Compressed air can be stored in underground cavities and start up fast with an uncomplicated converter system to produce electricity with efficiency up to 60-70% [6] and a high energy density of 0.2-2 MJ/kg [1]. In order to convert the energy stored in compressed air, gas turbines are used to run a generator to produce electricity [5]. Air motors are rarely used as energy-consuming components in current technological solutions. Depending on the size, CAES systems are modelled differently. There are various kinds of CAES systems: low temperature, isothermal or adiabatic compressed air energy storage [15],[18],[19].

Due to slight temperature changes, small systems are designed as isothermal, so-called i-CAES [2].

Adiabatic systems with low operating temperatures are also being investigated to improve energy conversion efficiency. Usage of multistage radial compressors and expanders can lead to system efficiency of around 55%. [11].

CAES can be designed differently to work in various combined systems, e.g. with a wind turbine connected directly or in a hybrid way [16].

Efficiency gains can also be developed with better energy utilisation efficiency. The Huntorf power plant was the first CAES plant commissioned to surplus energy during off-peak periods. The diabatic CAES

running on compressed air at around 72 bar pressure achieved a capacity of 290 MW. The Huntorf CAES plant uses a high-pressure gas turbine with a fast start-up capability to utilise stored energy [3]. The micro-CAES studied in [4] achieved a total efficiency of 45% with an electrical output of 3.5~kW. The authors cited that the greatest challenges were the high angular velocity and mechanical and electrical losses between the generator and turbine [4]. Another huge CAES power plant in McIntosh, USA, generating 110 MW of power, stores compressed air in underground caverns. With storage pressures of up to 7.5~MPa and a heat recovery system, the power plant uses 25% less fuel than the Huntorf plant [5]. The lack of evolution of the existing utilisation system can be seen in CAES literature research.

Turbines [23], [24] and air engines [25] can be distinguished as the utilisation element of CAES systems.

This paper presents the development of a utilisation component such as a low-pressure compressed air engine. Compressed air engines can be used as a propulsion system in a vehicle [9] and are also used in food, packaging, aerospace and many other industries.

The pneumatic motor has many advantages, such as small size, high torque, low cost and convenient operation [9]. Researchers have analysed the effect of intake and injection parameters and their impact on engine performance. The device's maximum power was obtained by changing the size of the injector and flywheel [28].

Unfortunately, a considerable disadvantage of pneumatic machines is their low energy efficiency [8]. The heat supply used to warm up the cylinder can improve the engine's overall performance by 8% [7]. Therefore, we will not observe a significant increase in efficiency with the use of heat recovery on small systems due to minor temperature differences.

The conducted research is based on the relationship between the increase in efficiency and the number of engine pistons driving the generator. An integrated air motor and constant load generator system have been modelled. The system's appropriate geometrical values and initial parameters were selected through simulation for the entire energy utilisation system to function as efficiently as possible. The design of the air injection system, stroke size, and generator load selection analysis were undertaken to achieve the highest efficiency, i.e., the highest power output and the lowest compressed air consumption.

1. THEORETICAL BACKGROUND

Compressed air is utilised to do work and move the engine piston. The moving piston sets the crankshaft in motion, which drives the generator's shaft. It was noted in [8] that generated force should be twice the load, primarily because of leakages and heat transfer CA system losses.

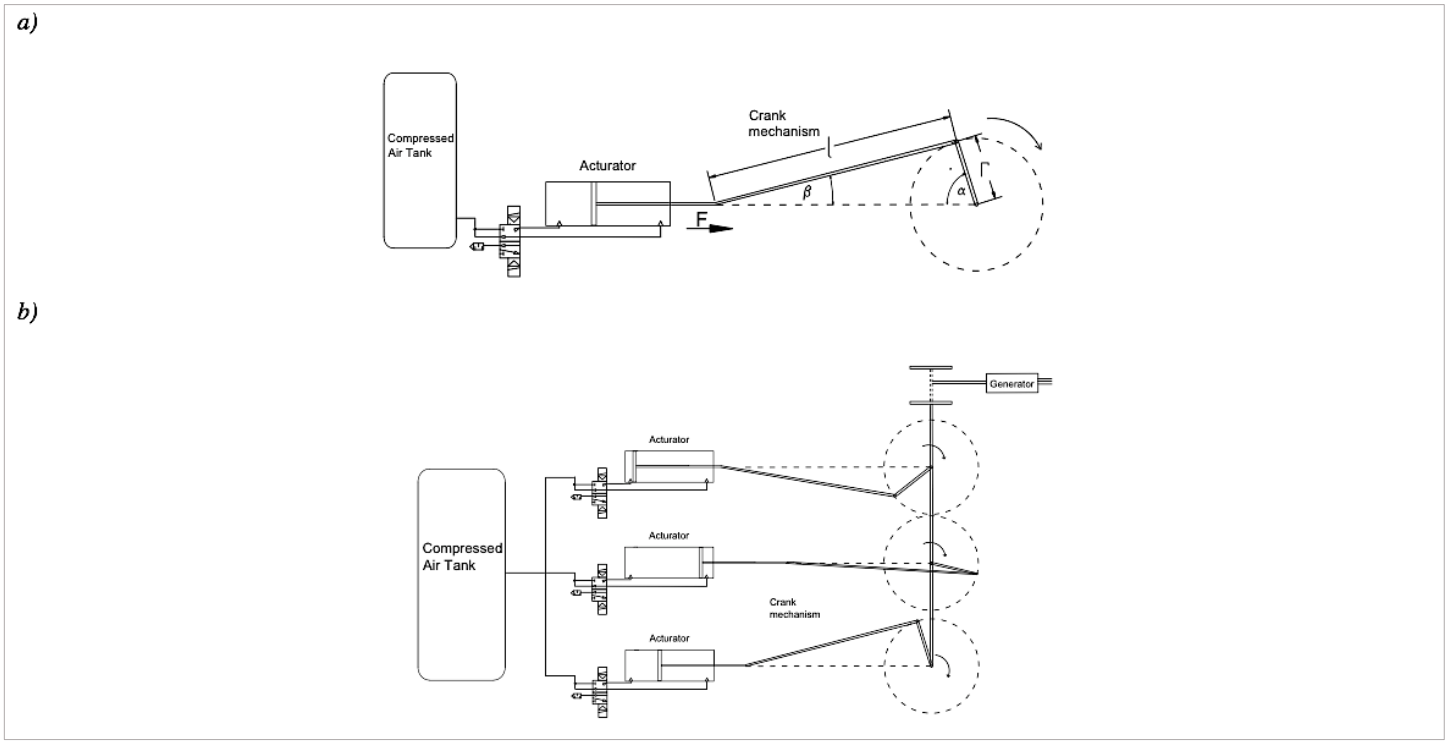

Fig. 1 Topology of compressed air engines: a) topology of a single-cylinder engine b) three-cylinder engine scheme.

Fig.1a shows the topology of a single actuator engine. The scheme was the basis for describing the mathematical relationships of the piston movement and converting its linear movement into rotational shaft movement. The force F shown in Fig. 1a is the force that pushes the piston in the cylinder. The angles alpha and beta symbolise the crank rotation angle marked as *r* and connecting the rod marked as *l*.

Fig.1b presents the author's solution for a multi-piston compressed air engine. In our approach, the three-cylinder engine is constructed as a set of three correspondingly smaller actuators. Actuators with a 120-degree different initial position drive the shared shaft.

Both systems cooperate with an isochoric compressed air tank. Despite the presented research on improving the system's functioning cooperating with an isobaric tank [13], it was decided to present isochoric tanks on the diagrams because the work does not focus on the selection of the tank, the impact of which on the engine's operation is negligible.

The mechanical work of the piston was converted into electricity through a generator connected to the shaft by a set of mechanical transmissions. A belt transmission connects the shaft with the T90 and T32.

The system of ordinary differential equations is written as follows:

$$\begin{cases} \frac{d\alpha}{dt} = \omega \\ \frac{d\omega}{dt} J = M - M_F - M_G \\ L_g \frac{dI}{dt} = N_{pb}\omega\Psi - (R + R_g)I \end{cases} \quad (1)$$

Where α - crank angle, *t* - time, ω - rotary speed of a shaft, *J* - moment of inertia, *M* - driving torque, M_F - frictional torque, M_G - generator torque, *I* - current, N_{pb} - poles number, Ψ - magnetic flux in air gap, *R* - load resistance, R_g - stator winding resistance of PMSG, *Lg* - stator winding inductance of PMSG.

The torque dependencies for each actuator are written as below based on Fig. 1

$$M(t) = rF(\cos(\alpha(t))\sin(\beta(t))\cos(\beta(t)) - \sin(\alpha(t))\, cos^2(\beta(t)) \quad (2)$$

Where *r* is the length of the crank arm, *F* is the force pushing the piston, α is the crank angle, and β is the connecting rod angle.

Generator torque is calculated as follows:

$$M_G = \frac{3}{2} I\varphi N_{pb} \quad (3)$$

According to [29] the braking torque of the bearing for a more precise calculation needs to be divided into two components: load-dependent and load-independent:

$$M_F = M_0 - M_1 \quad (4)$$

$$M_{Ind} = f_1 P_{eq} d_m \quad (5)$$

$$M_{dep} = f_0(\nu\omega)^{\frac{2}{3}} d_m 10^{-7} \quad (6)$$

Where f_0 is the factor depending on the type and size of the bearing and the type of lubrication, f_1 is the factor depending on the type and size of the bearing and the acceptable static load factor; d_m is the bearing pitch diameter, *v* is the kinematic viscosity of the oil, P_{eq} is the equivalent load.

Depending on the direction of piston movement, the force driving the piston is calculated as follows

$$Fp = \begin{cases} p_1 A_1 \text{ for } \alpha \geq 0\ i\ \alpha < \pi \\ -p_2(A_1 - A_2) \quad \text{for} \quad \alpha > \pi\ i\ \alpha < 2\pi \end{cases} \quad (7)$$

Where p_1 is the supply pressure in the first chamber of the cylinder, $p_2\ is$ the supply pressure in the second chamber of the cylinder, A_1 is the piston surface, A_2 is the piston rod surface.

The Coulomb-Viscous friction force acting on the piston in the cylinder, according to the authors [30], is described below

$$F_T = -\text{sgn}(\text{u})(N(\mu_2 + (\mu_1 + \mu_2)e^{-|\text{u}|}) + (\mu_3|\text{u}| + \mu_4|\text{u}|^2)) \quad (8)$$

Where $\imath$ is the piston velocity, μ_1 is the static friction coefficient, μ_2 is the dynamic friction coefficient, μ_3, μ_4 is the viscous friction coefficient, *N* is the piston contact force

Driving torque is estimated as a sum of the driving torques of the entire system.

$$\sum_{i=1}^{n} M_i = M_1 + M_2 + \ldots + M_n \quad (9)$$

Where n is the number of actuators in the system and $M_{1,2,..,n}$ is the driving torque of each 1,2,…,*n* actuator.

The moment of inertia is estimated as a sum of the moments of inertia of the entire system.

$$\sum_{i=1}^{n} J_i = J_1 + J_2 + \ldots + J_n \quad (10)$$

Where n is the number of actuators in the system and $J_{1,2,...,n}$ is the moment of inertia of each 1,2,…,*n* actuator.

In order to calculate efficiency, energy of compressed air has been calculated as:

Compressed air power [8]

$$P_{air} = p_A \dot{V} ln\frac{p_A}{p_0} \quad (11)$$

Where p_A is the supply pressure, $\dot{V}$ is the volumetric expenditure, p_0 is the absolute pressure.

In paper [9], engine power was described as:

$$P = \frac{2\pi\omega M_d}{6} \quad (12)$$

Where M_d is the driven torque, ω is the rotary speed.

In our case, we gain electricity as an end product of the system. The power generated by the generator is estimated as:

$$P_{gen} = I(\mathrm{R} + R_g)^2 \quad (13)$$

Where *I* is the current, *R* is the load resistance, R_g is the stator winding resistance of PMSG.

Total efficiency is defined as the quotient of the power produced by the generator and the compressed air energy

$$\eta = \frac{P_{gen}}{P_{air}} \quad (14)$$

In our approach, a three-cylinder engine is constructed as a set of three correspondingly smaller actuators. Actuators with 120 degrees different initial positions drive the shared shaft.

The Multi-piston system will stabilise the generated power, which may result in better system efficiency. The presented research is aimed at comparing the power of single-cylinder and three-cylinder engines and analysing sensitivity of the multi-piston system.

2. RESULTS

In order to investigate the performance of the air engine, a mathematical model was made in MatLab software, in which the engine operation process takes place. The low-pressure air motor, the results of which are presented below, operated with a supply pressure of 3 bar.

2.1 Model validation

First, to validate the program, the results of one piston engine (blue) were compared to the experimental survey (green), as shown in fig.2 and fig.3. Both engines have a stroke and a cylinder diameter of 200mm. The comparison covered the shaft rotation speed, pressure changes in the cylinder chambers and the power generated by the generator.

The main parameters of CAE used in the experiment and modelled in MatLab are shown in tab.1:

Parameter	Value	Unit
Engine stroke	0.2	m
Cylinder diameter	0.*2*	m
Crank length	0.1	m
Crankshaft length	0.46	m
Supply pressure	3	bar

Tab.1 Validation engine parameters

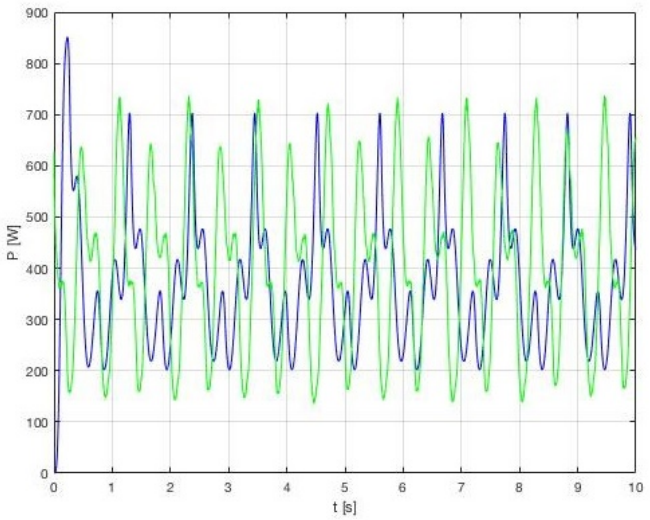

Fig.2 Generated electric power.

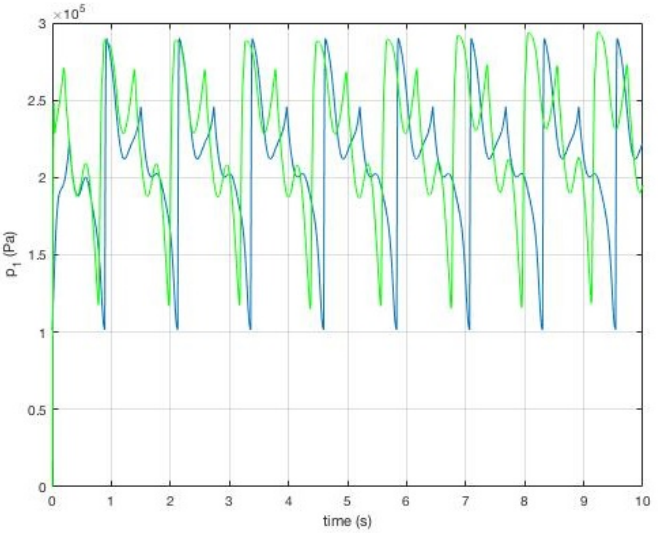

Fig. 3 Pressure in one of the chambers of the cylinder.

The average power in *t*=10s from the experimental date is 401.96 W. Average power in *t*=10s from the model results date is 374.72 W. The difference between the results equals 6.77 %. During the operation of a single actuator, we can observe the irregularity of the generated power related to the jumps in shaft rotational speed.

2.2 *One-piston and three-piston engine performance comparison*

The main parameters of three-piston CAE modelled in MatLab are shown in tab.2:

Parameter	Value	Unit
Engine stroke	0.2	m
Cylinder diameter	0.067	m
Crank length	0.1	m
Crankshaft length	0.46	m
Supply pressure	3	bar

Tab.*2* Three-piston *engine parameters.*

Further calculations were carried out for three actuators with a stroke of 200mm and a diameter of 67mm.

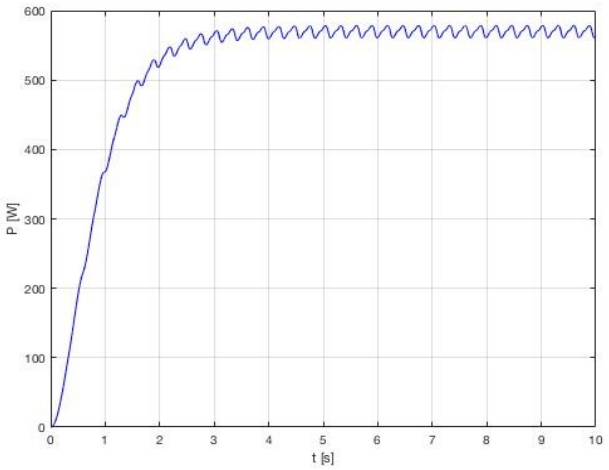

Fig. 4 Generated electric power – three-cylinder engine.

Fig 5. and Fig. 6 show the air mass consumption as a function of angle change.

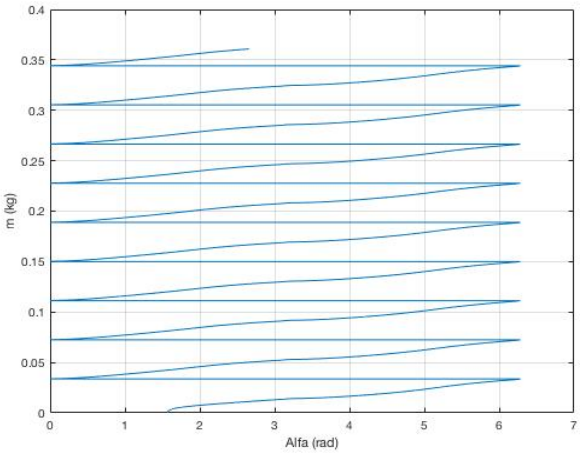

Fig.5 Air mass consumption in a single-cylinder system as a function of the crank angle change.

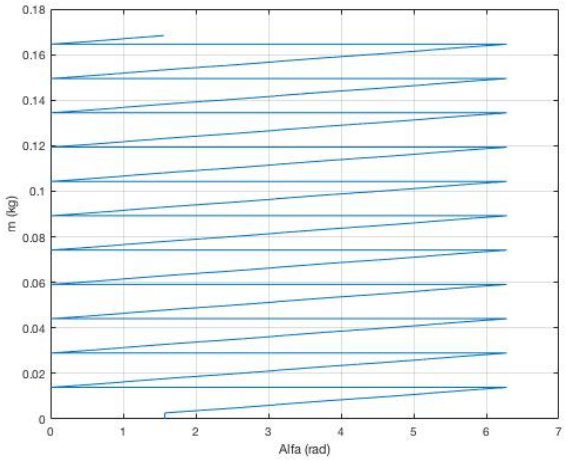

Fig. 6 Air mass consumption in a three-cylinder system as a function of crank angle change.

The air consumption for 10 seconds of engine operation is 0.36 kg for the single-cylinder engine and 0.168 kg for a three-cylinder engine.

The average power generated by 3 actuators is 518W. Although we use smaller cylinders, we get higher average power and only slight oscillations in the power value after a short time of stabilisation of the engine system.

2.3 Sensitivity analysis

In order to check the best possible engine performance, it was decided to carry out a series of simulations for various values of parameters, such as:

- generator load
- size of inlet connections
- actuator stroke length.

A series of simulation loops were run to study the effect of generator load on the delivered electrical power. The changing parameter was the generator load. Simulations were performed for supply overpressures of 1.9, 3, 5 and 7 bar.

.

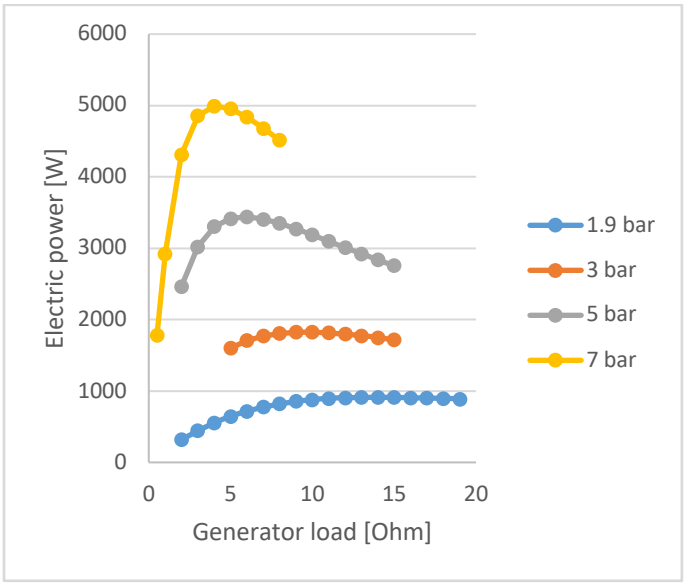

Fig. 7 Plot of the power generated by the generator as a function of generator load for four values of supply overpressure.

Maximum power can be obtained with proper selection of the generator load individually for each system. It was proven that we would obtain the highest power at a different resistance value with varying values of the supply pressure.

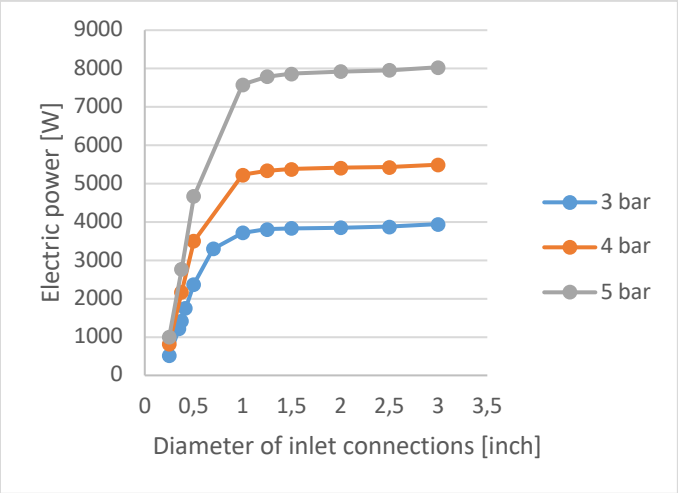

Fig. 8 Plot of the power generated by the generator as a function of the inlet connections diameter for three values of supply overpressure

The size of inlet connections has a direct impact on engine performance. By increasing the diameter of the stub pipe, the power increases to a certain point and reaches its maximum. We observe only slight changes in power values as the diameter of the inlet stubs increases.

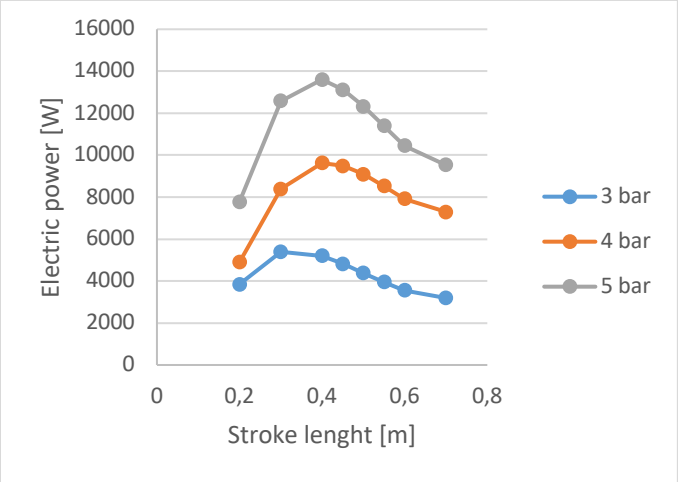

Fig. 9 The plot of electric power as a function of actuator stroke for three values of supply overpressure.

Each system, depending on the selected initial parameters and geometrics, requires the stroke size to be selected to obtain the highest power and efficiency gain.

2.4 Engine performance for the modelled air injection system working with 8 bar supply overpressure.

The solution proposed by the authors of the work was a compressed air injection system in which the power supply is disconnected when the piston is at the mid-stroke of the actuator, due to its speed and the further expansion of the air, the piston moves by the entire length of the cylinder. Not only is air consumption reduced, but the smaller amount of air also facilitates air expulsion when the piston changes direction.

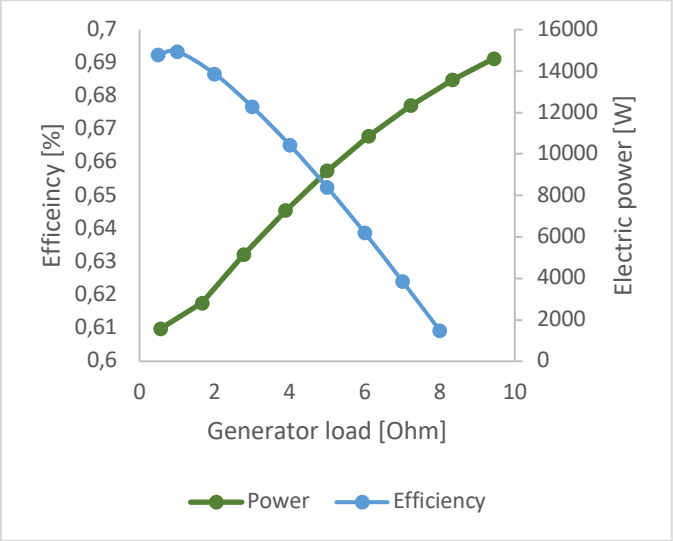

Fig.10 Efficiency and electric power as a function of generator load for 8 bar value of supply overpressure working with the authors' innovative air injection system.

The highest efficiency of 69% was obtained for a 1ohm value of generator load but only with 2806 W of electric power.

3. CONCLUSION

By using more cylinders, better performance of the air engine can be achieved. The average power of a three-cylinder engine is 27% higher than that of a single-cylinder engine. The presented engine also uses 53% less compressed air than the popular single-cylinder compressed air engine. Further research consisting of the appropriate selection of the generator parameters and the physical sizes of the actuators may lead to even higher efficiency of the air engine utility component for CAES systems.

Sensitivity analysis has proven that by selecting appropriate initial and geometrical parameters of the engine, we are able to achieve better engine performance. The computer model is a design map and can be used in the design of compressed air engines. Estimating the power we need or the amount of compressed air we have, we can perfectly match the engine parameters to our needs and capabilities.

The air injection system presented by the authors led to a 69% engine efficiency at low generator load. Further research consisting in making a prototype and further research on the selection of parameter values and the air injection system development may lead to even greater savings and higher efficiency of the energy utilisation system stored in compressed air.

ACKNOWLEDGEMENT

The work was carried out as part of a research subvention under contact no. 16.16.210.476 supported by the Polish Ministry of Education and Science.

REFERENCE

[1] MS Guney, Y. Tepe, Classification and assessment of energy storage systems, Renew. Sustain. Energy Rev. 75 (2017) 1187–1197.
[2] Abdul Hai Alami. Experimental assessment of compressed air energy storage (CAES) system and buoyancy work energy storage (BWES) as cellular wind energy storage options.Journal of Energy Storage, Volume 1, 2015, Pages 38-43.
[3] Marcus Budt, Daniel Wolf, Roland Span, Jinyue Yan. A review on compressed air energy storage: Basic principles, past milestones and recent developments, Applied Energy, Volume 170, 2016, Pages 250-268.
[4] Thales A.C. Maia, Jos. E.M. Barros, Braz J. Cardoso Filho, Matheus P. Porto. Experimental performance of a low cost micro-CAES generation system. Applied Energy, Volume 182, 2016, Pages 358-364.
[5] Haisheng Chen, Thang Ngoc Cong, Wei Yang, Chunqing Tan, Yongliang Li, Yulong Ding,
Progress in electrical energy storage system: A critical review. Progress in Natural Science, Volume 19, Issue 3, 2009, Pages 291-312.
[6] T.L. Brown, V.P. Atluri, J.P. Schmiedeler, A low-cost hybrid drivetrain concept based on compressed air energy storage, Applied Energy, Volume 134, 2014, Pages 477-489.
[7] Yidong Fang, Yiji Lu, Xiaoli Yu, Anthony Paul Roskilly, Experimental study of a pneumatic engine with heat supply to improve the overall performance, Applied Thermal Engineering, Volume 134, 2018, Pages 78-85.
[8] J.S. Leszczynski, D. Grybos, Compensation for the complexity and over-scaling in industrial pneumatic systems by the accumulation and reuse of exhaust air, Applied Energy, Volume 239, 2019, Pages 1130-1141.
[9] Yonghong Xu, Hongguang Zhang, Fubin Yang, Liang Tong, Dong Yan, Yifan Yang, Yan Wang, Yuting Wu, Experimental research on universal characteristics and output performance of pneumatic motor for compressed air vehicle, Journal of Energy Storage, Volume 41, 2021, 102943.
[10] Daniel Wolf, Marcus Budt, LTA-CAES – A low-temperature approach to Adiabatic Compressed Air Energy Storage, Applied Energy,Volume 125,2014,Pages 158-164.
[11] Henrik Lund, Georges Salgi, The role of compressed air energy storage (CAES) in future sustainable energy systems, Energy Conversion and Management, Volume 50, Issue 5,2009, Pages 1172-1179.
[12] Bartosz Stanek, Jakub Ochmann, Łukasz Bartela, Michał Brzuszkiewicz, Sebastian Rulik, Sebastian Waniczek, Isobaric tanks system for carbon dioxide energy storage – The performance analysis, Journal of Energy Storage,Volume 52, Part A,2022,104826.
[13] Tong, Zhengren & Wang, Hu & Xiong, Wei & Ting, David & Carriveau, Rupp & Wang, Zhiwen. (2021). Accumulated and transient exergy analyses of pneumatic systems with isochoric and isobaric compressed air storage tanks. Energy Storage. 3. 10.1002/est2.269.
[14] Andrew J. Pimm, Seamus D. Garvey, Maxim de Jong, Design and testing of Energy Bags for underwater compressed air energy storage,Energy, Volume 66, 2014, Pages 496-508.
[15] Hyrzyński, Rafał & Ziółkowski, Paweł & Kruk-Gotzman, Sylwia & Kraszewski, Bartosz & Badur, Janusz. (2019). Thermodynamic analysis of the Compressed Air Energy Storage system coupled with the Underground Thermal Energy Storage. E3S Web of Conferences. 137. 01023. 10.1051.
[16] Mazlan, Abid. (2020). Compressed Air Energy Storage System for Wind Energy: A Review. International Journal of Emerging Trends in Engineering Research. 8. 3080-3087. 10.30534/2020/34872020.
[17] Shuyu Zhang, Huanran Wang, Ruixiong Li, Chengchen Li, Fubin Hou, Yue Ben, Thermodynamic analysis of cavern and throttle valve in large-scale compressed air energy storage system, Energy Conversion and Management, Volume 183, 2019, Pages 721-731.
[18] Youssef Mazloum, Haytham Sayah, Maroun Nemer, Dynamic modeling and simulation of an Isobaric Adiabatic Compressed Air Energy Storage (IA-CAES) system, Journal of Energy Storage, Volume 11, 2017, Pages 178-190.
[19] Ruixiong Li, Huanran Wang, Haoran Zhang, Dynamic simulation of a cooling, heating and power system based on adiabatic compressed air energy storage, Renewable Energy, Volume 138, 2019, Pages 326-339.
[20] Massimo Guarnieri, Introduction to Electrochemical Energy Storage, Editor(s): Luisa F. Cabeza, Encyclopedia of Energy Storage, Elsevier, 2022, Pages 236-249.
[21] Mehdi Mehrpooya, Pouria Pakzad, Introducing a hybrid mechanical – Chemical energy storage system: Process development and energy/exergy analysis, Energy Conversion and Management, Volume 211, 2020, 112784.
[22] Mingxuan Guo, Yunfei Mu, Hongjie Jia, Youjun Deng, Xiandong Xu, Xiaodan Yu,
Electric/thermal hybrid energy storage planning for park-level integrated energy systems with second-life battery

utilization, Advances in Applied Energy, Volume 4, 2021, 100064.
[23] Ambra Giovannelli, Luca Tamasi, Coriolano Salvini, Performance analysis of industrial steam turbines used as air expander in Compressed Air Energy Storage (CAES) systems, Energy Reports, Volume 6, Supplement 1, 2020, Pages 341-346.
[24] A.G. Olabi, Tabbi Wilberforce, Mohamad Ramadan, Mohammad Ali Abdelkareem, Abdul Hai Alami, Compressed air energy storage systems: Components and operating parameters – A review, Journal of Energy Storage, Volume 34, 2021, 102000.
[25] Jin-Long Liu, Jian-Hua Wang, Thermodynamic analysis of a novel tri-generation system based on compressed air energy storage and pneumatic motor, Energy, Volume 91, 2015, Pages 420-429.
[26] Yuan Zhang, Ke Yang, Xuemei Li, Jianzhong Xu, The thermodynamic effect of air storage chamber model on Advanced Adiabatic Compressed Air Energy Storage System, Renewable Energy, Volume 57, 2013, Pages 469-478.
[27] Baoying Peng, Liang Tong, Dong Yan, Weiwei Huo, Experimental research and artificial neural network prediction of free piston expander-linear generator, Energy Reports, Volume 8, 2022, Pages 1966-1978.
[28] A Gupta, H Kathpalia, H Aggarwal, N. Kumar, Performance Based Optimization of Intake and Injection Parameters of an Advanced Compressed Air Engine Kit, 2017. SAE Technical Paper 2017-01-1291.
[29] S. Adamczak, R. Domagalski, E. Sender, Moment Oporowy W Łożyskach Tocznych– Metody I Urządzenia Badawcze, 2011, p. 21-22.
[30] J.S.Leszczynski, D.Grybos, Sensitivity analysis of Double Transmission Double Expansion (DTDE) systems for assessment of the environmental impact of recovering energy waste in exhaust air from compressed air systems, Applied Energy, Volume 278,2020,115696.